SCIENCE SET
OPEN ACCESS PUBLISHERS

Research Article

World Journal of Sensors Network Research

Design of High-Performance Graphene Lead Free Perovskite Solar Cells by Numerical Modeling Based on Coupled Differential Equations

Ladan, H.M. A[1*]., Adamu, A. S[2]., Buba, A.D. A[3]., & Umar A[4]

[1]*Department of Physics, Faculty of Science, Sa'adu Zungur University, Bauchi State, Nigeria*
[2]*Department of Electrical Engineering, Ahmadu Bello University, Zaria, Nigeria*
[3]*Department of Physics, Faculty of Science, University of Abuja, Abuja*
[4]*Department of Chemistry, Faculty of Science, University of Abuja, Abuja, Nigeria*

[*]**Corresponding author:** Ladan HMA, Department of Physics, Faculty of Science, Sa'adu Zungur University, Bauchi State, Nigeria.

Submitted: 30 November 2024 **Accepted:** 06 December 2024 **Published:** 15 January 2025

Citation: *Ladan, H. M. A., Adamu, A. S., Buba, A. D. A., & Umar, A. (2025). Design of high-performance graphene lead-free perovskite solar cells by numerical modeling based on coupled differential equations. Wor Jour of Sens Net Res, 2(1), 01-09.*

Abstract

In this study, graphene was prepared by modified Hummer's method and the optical properties were explored using UV-visible spectroscopy to determine absorption coefficients at different wavelengths based on Beer-Lambert's law. In the second step, graphene based lead-free methyl ammonium germanium halide solar cell was designed using GO as carrier transporters. Numerical modelling of the device in solar capacitance stimulating (SCAPS 1D) program based on second order differential equation was done. A 0.6227 V, 38.58 mAcm-2, 83.07 %, 19.95 % were recorded as the open-circuit voltage, current density, fill factor and power conversion efficiency for FTO/GO/Perovskite/Cu2O/Au. The investigation showed that the presence of graphene improved the optical transparency and enhanced carrier generation and interaction between other layers which optimized the electrical conductivity and efficiency of the solar cells when compared to previous studies in literature. The results emphasized a viable approach to in the design of efficient and stable solar cells at a reduced cost and optical losses. If mass produced can deployed in Africa due to massive solar energy potential.

Keywords: Optical Property, Graphene, Perovskite, Solar Cells, SCAPS, Numerical Modeling

Introduction

Due to increasing energy demand worldwide, studies on improving the performance of photovoltaic (PV) devices are on the increase [1]. Integration of carbon-based material in designing solar cells improved efficiency, reduced cost and enhanced life time [2]. Graphene is a single layer of graphite and is sp2 hybridized carbon atoms in hexagonal form. It has high electronic conductivity at room temperature. The thermal conductivity is 3.0×103 Wm/K and the transmittance is about 90% [3, 4]. Graphene oxide (GO) has carboxyl, epoxy and hydroxyl functional groups [5]. It has very large surface area (2630 m2/g).

Perovskite material can be represented by the formula ABX3 where A is a cation (A+), an organic methyl ammonium (MA), formamidinium (FA) or Cesium (Cs) ions. B is a heavy metal such as Pb, Ge or Sn, while X- is a halide anion (I, Br, Cl, or their mixtures). Perovskite solar cells (PSCs) suffers from drawbacks due to low electron mobility in the metallic semiconducting components (SMOx) such as TiO2, SnO2 and ZnO with a higher density of electronic trap states, instability under UV visible light, poisonous lead, hysteresis, and operational life-time. The excessive energy loss due to the transmission and thermalization of hot carriers can be minimized by sandwiching carbon or polymers in between the layers [6, 7]. The development of lead-free PSCs is in progress. Carbon based GO improves the performance of PV devices by enhancing the photo-generated electrons since the carbon molecules absorb light energy in the UV-visible range at different wavelengths [8]. Adding absorption coefficient (α) profile into photovoltaic (PV) devices at UV-visible range from 200 nm to 800 nm is vital for the optimum performance of optoelectronic and PV cells [8, 9].

Pulson's group in 2003 performed an optical characterization of Cu (In,Ga)Se2 (CIGS) alloy thin films by spectroscopic ellipsom-

etry technique [10, 11]. extrapolated the absorption coefficients of the Cu (In,Ga)Se2 from Pulson's study for the simulation of chalcopyrite dual-junction based tandem solar cells. The result showed a strong correlation between its bandgap and efficiency. Several studies on PSCs [12, 13]. have been performed without adding the absorption coefficient (α) profile to the device. It is known that optical properties of nanomaterials are enhanced by the nature of the band gap, absorption coefficient, and carrier diffusion length (100-1000 nm) [14, 15]. This can improve the carrier transport, and the photovoltaic parameters [16, 17]. There were no records on the measurement and incorporation of the absorption data into photovoltaic device especially GO in PSCs as absorber or transport layer [18-20].

In this study, GO was prepared by modified Hummer's method and the optical properties were explored using UV-visible spectroscopy to determine absorption coefficients at different wavelengths based on Beer-Lambert's law. The data were incorporated in the design of lead-free methyl ammonium germanium halide solar cell using GO as carrier transporters in SCAPS 1D program.

Materials and Methods

Materials

Synthetic graphite (Sigma Aldrich), H2SO4, NaNO3, HNO3, HCl, KMnO4, and distilled water. All the chemicals used were of analytical grade and were used without further purification. The fluorine doped tin oxide (FTO) glass substrates (Solaronix, Switzerland). The FTO, synthetic graphite and NaNO3 were ordered from their respective vendors.

Modified Hummer's Method

GO was synthesized by mixing 5 g of graphite powder and conc. H2SO4 and HNO3 in the ratio (3:1) in a 500 ml beaker and was sonicated for 30 min. 6 g of KMnO4 was added gradually and stirring continued in an ice bath for 30 minutes. Then the mixture was kept on a magnetic stirrer at 200 rpm and the temperature was increased to 30 0C. A brown colouration was formed. The temperature was raised to 80 0C and a bright-yellow suspension was formed. When 30 ml H2O2 (30%) was added, it changes to golden yellow solution. After centrifugation, dilute HCl was used to wash the resultant product and properly rinsed with deionized water. 0.5 g of the synthesized GO was annealed at 150 0C for 20 minutes (figure 1 a. and b.). 0.2 g was coated on gold substrate for characterization and subsequent production of GO thin films on FTO glass substrate (solaronix), the procedure was adopted from Ladan and Buba, 2021.

Optical Characterization and Simulation

The absorbance values of the GO were determined using UV visible spectrophotometer (T80+) at Nile University labouratory, Abuja to provide the data in the design of lead-free methyl ammonium germanium halides using GO as carrier transporter and optimizers for a hassle-free hole and electron transfers.

Solar Capacitance Stimulation

Numerical modeling was performed using SCAPS version 3.3.09 under AM 1.5 solar spectrum at 100 mW/cm2 light intensity to obtain the photovoltaic characteristics. SCAPS can simulate the electric field distribution, current density, transport properties, carrier generation and recombination profile for thin films solar cells [21]. The Poisson equation relates the static electric field ε to the space-charge density ρ. The electron and hole transport equations (2 and 3) are coupled by ε to form a set of coupled differential equations.

$$\frac{d^2\emptyset(x)}{dx} = -\frac{d\,\varepsilon(x)}{dx} = -\frac{\rho(x)}{\epsilon_0\epsilon_s} \quad (1)$$

Where o is the electrostatic potential, $E(0$)is the permittivity of free space and Es is the static relative permittivity of the medium.

$$D_e\frac{d^2n}{dx^2} + \mu_e\varepsilon\frac{dn}{dx} + n\mu_e\frac{d\varepsilon}{dx} - R_e(x) + G_e(x) = 0 \quad (2)$$

$$D_h\frac{d^2p}{dx^2} + \mu_h\varepsilon\frac{dn}{dx} + p\mu_h\frac{d\varepsilon}{dx} - R_h(x) + G_h(x) = 0 \quad (3)$$

Where e and p are the electron and hole densities, μ_e and μ_p represents the electron and hole mobilities, D_e and D_hare the electron and hole diffusion constants, R(x) and G(x) denotes the recombination and photo-generation rates, respectively.

As shown in figure 1c, the device is a thin film solar cell which was modelled as a stack of layers characterized by the thickness, doping level, charge mobility, absorption coefficient and other physical properties of the material. The two-configuration tested are FTO/GO/Perovskite/Cu2O/Au and FTO/GO/TiO2/Perovskite/Spiro-OMETAD/Au. The absorption coefficient was set at 105 cm−1 and the operating temperature at 300 K while that of GO was incorporated between 200 and 800 nm.

Table 1 shows parameters that were collected from recent studies. These include band gap energy (Eg), electron affinity (χ), relative dielectric permittivity (εr), mobility of electron (μn) mobility of hole (μp) and defect density (Ntm), Nc(cm-3) is effective density of states at CB, Nv (cm-3) is the effective density of states at VB, Nd (cm-3) is the donor density /density of p-type doping, NA (cm-3) is the acceptor density/ density of n-type doping, εr is the relative dielectric permittivity, μ_n (cm2c-1s-1) is the mobility of electron, μ_h (cm2c-1s-1) is the mobility of electron, Nte (cm/s) is the electron thermal velocity, Nth (cm/s) is the hole thermal velocity.

Light Transmittance and Heat Distribution Across the Device

To show the light transmittance and heat distribution across the device, originPro version 9.8.0200 was used for the heat distribution and contour map for the absorbance versus the wavelength of the radiation and the 2D heat map for the transmittance against wavelength.

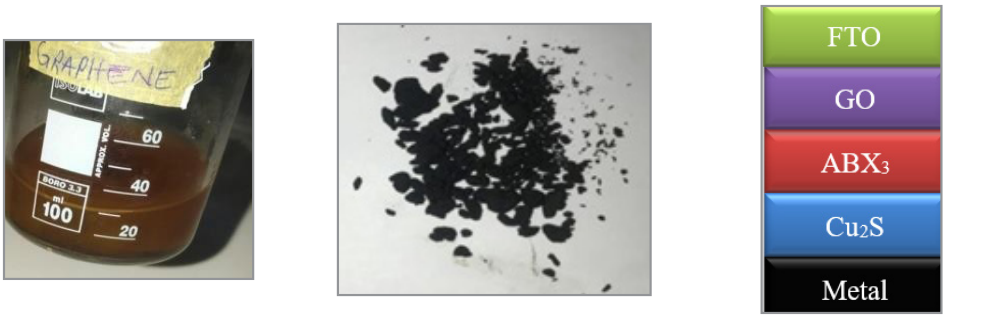

(a) (b) (c

Figure 1: Graphene in (a) Solution (b) Lump form (c) PSCs thin films

Results and Discussion

As shown in figure 1c, the device is a heterojunction (p-i-n) solar cell. Electrons are collected at the fluorine doped tin oxide (FTO) and holes at the metal with high work functions as back contact such as Au. The device has intrinsic perovskite absorber layer (non-doped) between an electron transport layer n-type GO and GO-TiO2 and hole transporting layer p-type Cu2O and Spiro OMeTAD with the absorption coefficient of GO incorporated the operating temperature at 300 K.

The optical absorbance coefficient of a semiconductor close to the band edge can be expressed by (1). The n depends on the nature of the transitions and the values can either be ½, 2, 3/2 or 3. It denotes allowed direct, allowed indirect, forbidden direct and forbidden indirect transitions respectively [22]. Here, n is 2 and GO thin films (Eg = 2.55 eV) were prepared on gold substrate, the absorption coefficient α can Be Expressed as:

$$\alpha(v)hv = B(hv\text{-}E_g)^n \quad (4)$$

Where B is constant ~ 1, α is the absorption coefficient, Eg is the energy band gap, n is between ½ and 3 depending on the transition [23, 24].

The measured absorption coefficient α(*t*) (cm-1) of GO at different wavelengths (Table 3) can be related to the transmittance (t) by

$$\alpha(t) = \frac{1}{d}\ln\frac{1}{t} \quad (5)$$

Where t = 10−A, d is the thickness of the thin film and A is the absorbance of the sample. The effect was observed from 200 nm to 800 nm at different wavelengths and absorption coefficient (α) in SCAPS software to record the photovoltaic characteristics (a) Efficiency of the device (b) Total recombination charges (Figure 2a and 2b).

The data in the design of lead-free methyl ammonium germanium halides using GO as carrier transporter and optimizers for a hassle-free hole and electron transfers. For the first configuration, a 0.6227 V, 38.58 mAcm-2, 83.07 %, 19.95 % were recorded as the open-circuit voltage, current density, fill factor and power conversion efficiency for FTO/GO/Perovskite/Cu2O/Au system and for the second configuration, FTO/GO/TiO2/Perovskite/Spiro-OMETAD/Au a 0.6659V, 10.77mAcm-2, 79.19%, 22.91% were obtained for the first time. The values showed enhanced photovoltaic parameters [25-27].

The presence graphene as contact /TCO layer improves the optical transparency since it can absorb 2.3% of incident light. It transfers 97% of incident light to the active layer which consequently leads to the increase in carrier generation and enhances the interaction between the other layers. This optimizes the electrical conductivity and efficiency of solar cells. The Electron transporting layer (ETL) plays a vital role in the exciton separation and charge transport. TiO2 is widely used as the ETL in PSCs. It has suitable band gap, excellent photo-electrochemical stability, and simple preparation process. The use of GO-TiO2 as ETLs films increase the charge collection efficiency and reduce recombination occurring at the interfaces [28-32]. Photovoltaic parameters obtained were compared with similar studies available in the literature (Table 2) [33-41].

The transmitted light and heat distribution showed the absorbance versus the wavelength of the radiation while the 2D heat map showed the transmittance against wavelength indicated peak heat generation at 700 nm/tr between 0.5 and 0.25 above violet at the same projection (700 nm) for the 3D surface plot. While polar contour in terms θ(x) r(Y) revealed possible angle that solar cell can be tilted to achieve maximum absorbance and transmittance at 550.5 nm (figure 6 and 7) [42-44].

Table 1: Material property for each layer of the PSCs

	ITO	Spiro-Ometad	FASnI3	TiO2	MAGeI3	Graphene
Thickness, nm	500	WR	WR		WR	WR
Eg(eV)	3.65	2.9	1.3	3.2	1.90	2.7
x (eV)	4.80	2.2	4.17	3.9	3.98	4.5

Nc(cm-3)	5.8 x1018	2.5x1020	1x1018	1019	1016	3.10 x 1019
Nv (cm-3)	1018	2.5x1020	1.0 x1019	1019	1015	3.10 x 1019
Nd (cm-3)	1020	-	-	1017	109	
NA (cm-3)	0	1x1018	-	-	109	0
εr	8.90	3	6.5	32	10	3.3
μ_n (cm2c-1s-1)	10.0	0.0021	1.6	162x103	16.20	15,000
μ_h (cm2c-1s-1)	10.0	0.0021	1.6	101x103	10.10	15,000
Defect density	-	-	1.6 x106		1014	1 x 1015
Work function	-	-	1.6 x106		-	4.0
References	Kumar et al, 2020; Rai et al, 2020	Zhao et al., 2018; Mandadapu et al., 2017	Mandadapu et al., 2017; Kanoun et al., 2019	Kanoun et al., 2019	Lakhdar et al, 2019	Sutar et al, 2012; Mudd et al, 2015; Wang et al, 2020

Table 2: Photovoltaic parameters of the solar cells compared with similar studies

Structure	Jsc (mA/cm2)	Voc (V)	FF (%)	PCE (%)	References
FTO/GO/Perovskite/Cu2O/Au	38.58	0.6227	83.07	19.95	This study
FTO/GO/TiO2/Perovskite/Spiro-OMETAD/Au	10.77mAcm-2	0.6659	79.19	22.91	This study
mTiO2+G/perovskite/GO/spiro OMeTAD	22.48	1.08	75.12	18.19	Lakhdar et al., 2019
FAPbI3-based Simulation	16.60	0.60	40.60	4.3	Karthick et al., 2020
FAPbI3 Experimental	20.60	1.10	47.40	11.5	
MAPbI3-based Simulation	23.34	1.15	70.31	18.92	Rai et al., 2020
MAPbI3-based experimental	22.30	1.11	74.50	18.40	Rao et al., 2016
CH3NH3PbI3-based experimental	18.20	0.93	71.20	12.10	Zhu et al., 2016
CH3NH3PbI3-based solar cell Simulation, TiO2	23.44	0.93	60.75	13.30	Agresti et al., 2016
P-graphene/CH3NH3PbI3/n-cSi	30.87	0.6879	84.31	17.90	Gagandeep et al., 2020

Table 3: Absorption coefficient *α(t)* (cm-1) of GO at different wavelengths and thicknesses

(nm)	GO(A)	t(GO)	(d = 50nm)	(d = 100nm)	(d = 200nm)
200	0.172	0.6730	7922320	3961160	1980580
300	0.667	0.2153	30722020	15361010	7680505
400	0.650	0.2239	29939000	14969500	7484750
500	1.472	0.0337	67800320	33900160	16950080
600	1.723	0.0189	79361380	39680690	19840345
700	1.761	0.0173	81111660	37331630	20277915
800	1.629	0.0235	75031740	37515870	18757935

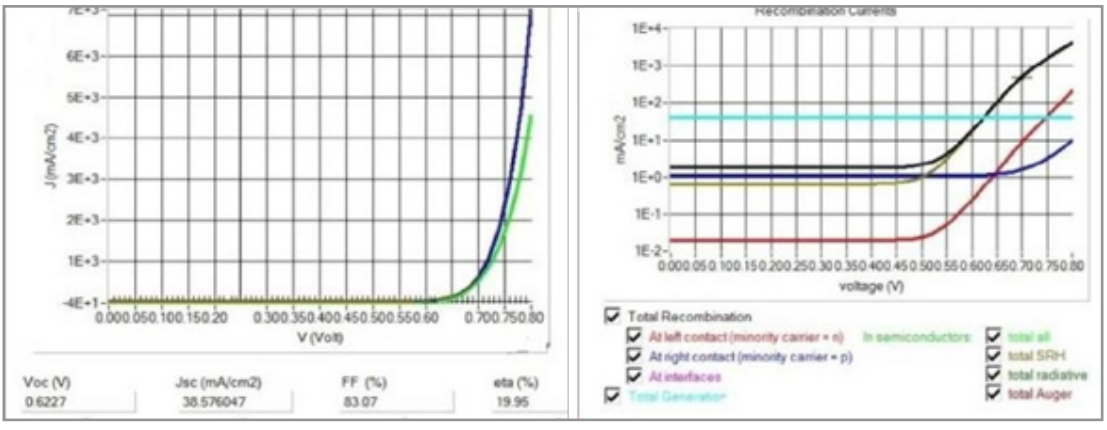

Figure 2: (a) Photovoltaic parameters of the first configuration and (b) recombination currents

For the second design, the Au/spiro-ometad/FASnI3/TiO2/FTO the current density increases sharply from 0.50 V (figure 3a.) and with valence and conduction band at -0.35 eV and 1.78 eV (figure 3b.) The occupation probability of deep defect for electrons and the carrier density is showed in figure 4. The generation and recombination profile recorded peak at 1.0µm, electron capture (dark), peak electron-hole generation (green), hole and electron emission (pink and blue) (figure 5). The optical absorption of the ITO/FTO layer and the J-V characteristics curve for second configuration are indicated in Figure 8.

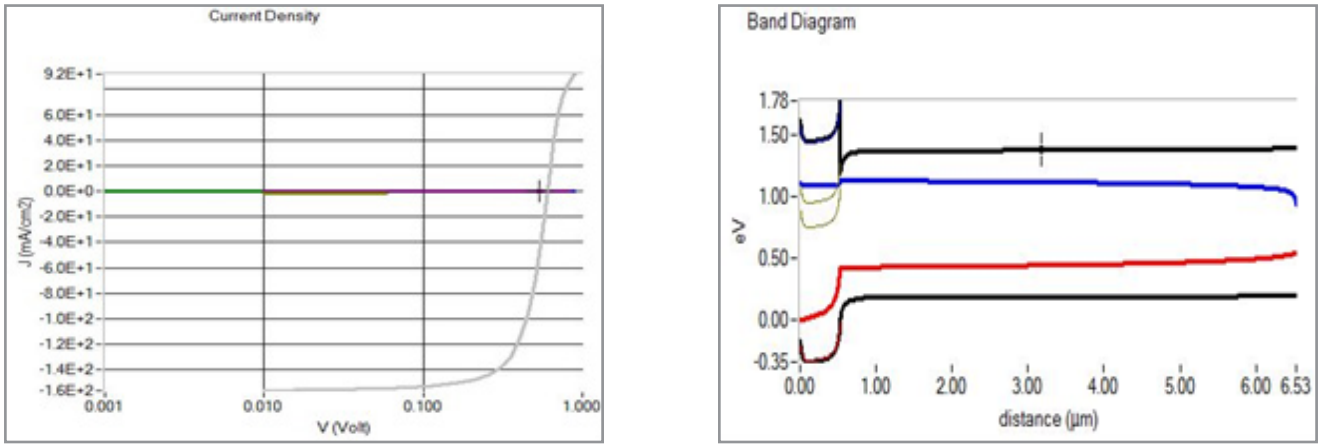

Figure 3: The current density and energy band diagram

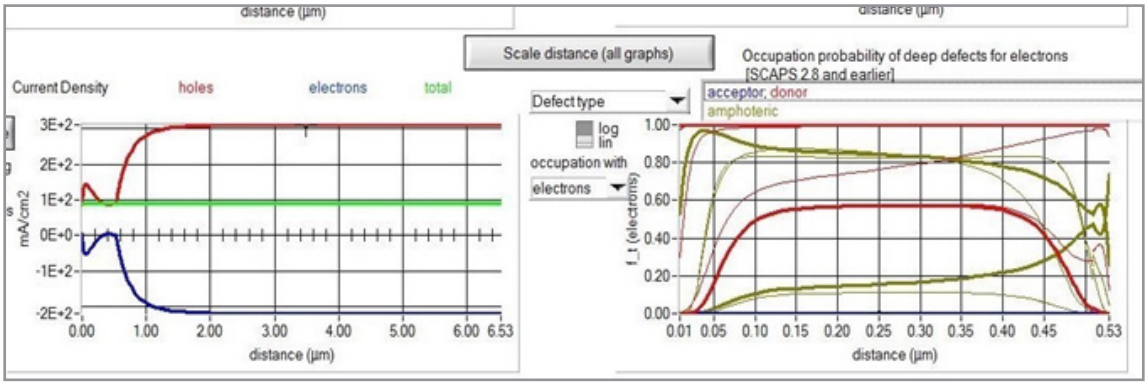

Figure 4: The occupation probability of deep defect for electrons and the carrier density

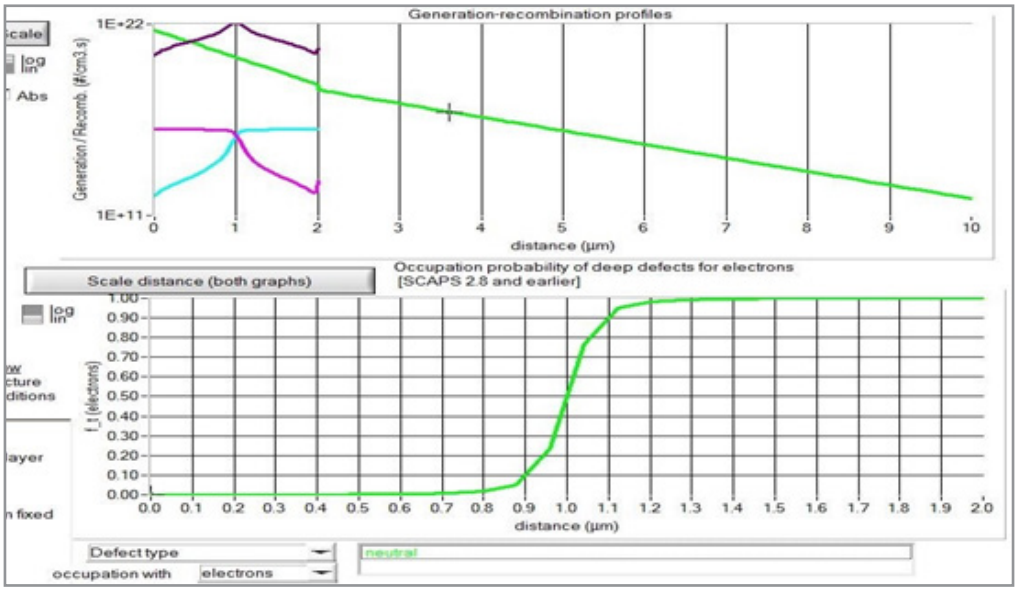

Figure 5: Generation and recombination profile

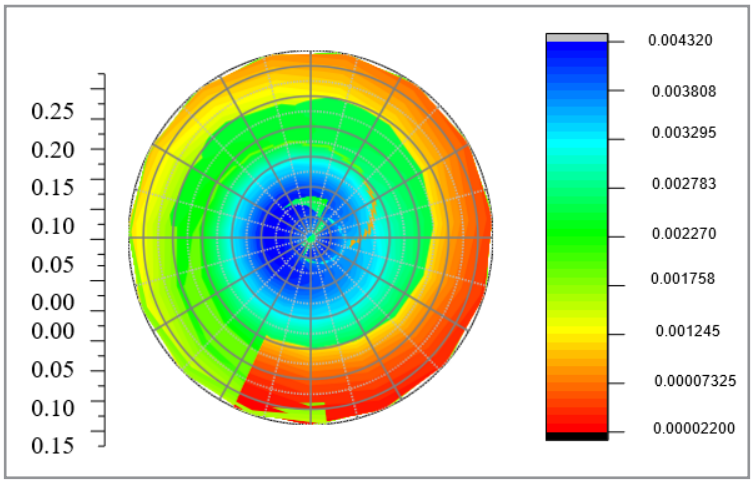

Figure 6: Polar contour: θ(x) r(Y)

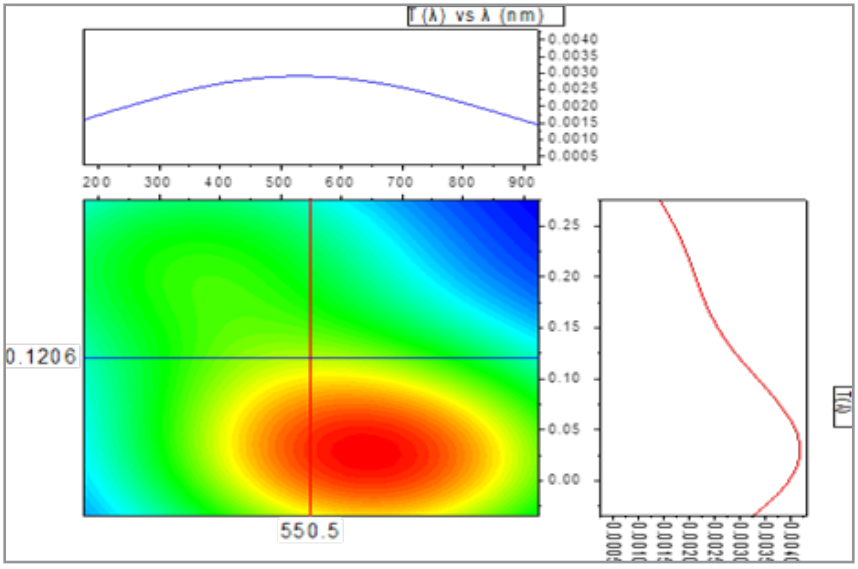

Figure 7: The maximum transmittance at 550.5 nm

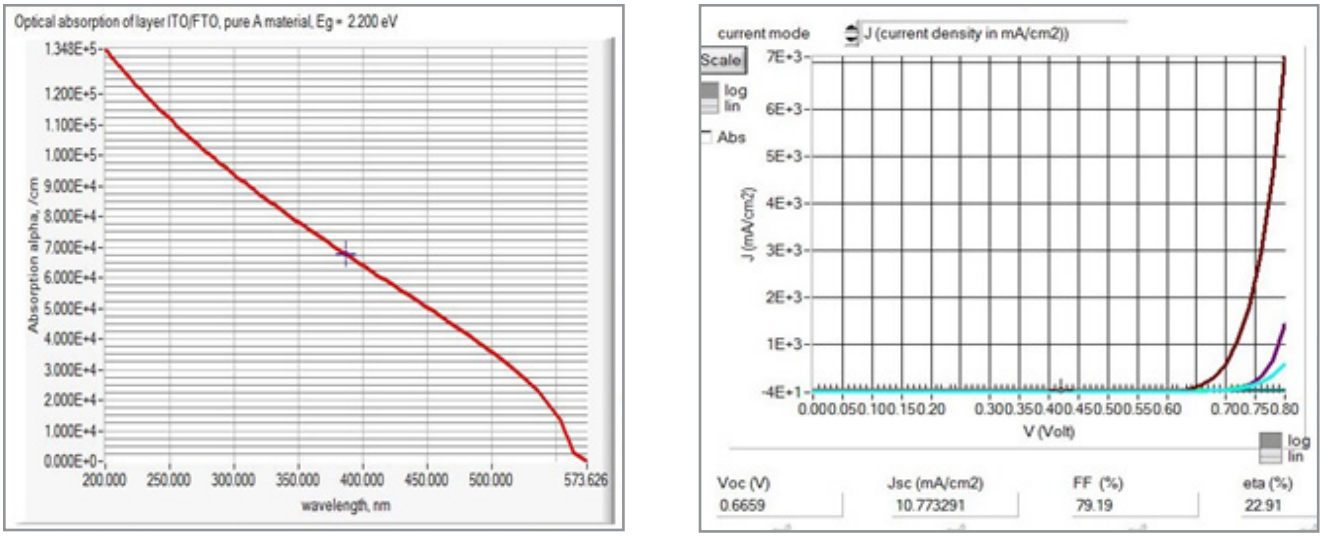

Figure 8: The optical absorption of the ITO/FTO layer and the J-V characteristics curve for second configuration.

Conclusion

In this paper, graphene oxide (GO) was synthesized by modified Hummer's method and the optical properties were explored using UV-visible spectroscopy. The absorption coefficients at different wavelengths based on Beer-Lambert's law were determined and used in the design of lead-free methyl ammonium germanium halide solar cell using GO as carrier transporters. The numerical modelling of the device in SCAPS 1D program based on second order differential equation was carried out. For the first time, a 0.6227 V, 38.58 mAcm-2, 83.07 %, 19.95 % were recorded as the open-circuit voltage, current density, fill factor and power conversion efficiency for FTO/GO/Perovskite/Cu2O/Au and FTO/GO/TiO2/Perovskite/Spiro-OMETAD/Au based design recorded 0.6659V, 10.77mAcm-2, 79.19%, and 22.91% respectively.

The investigation showed that the presence of graphene improved the optical transparency and enhanced carrier generation and interaction between other layers which optimizes the electrical conductivity and efficiency of the solar cells when compared to previous studies in literature. The results emphasized a viable approach to in the design of efficient and stable solar cells at a reduced cost and optical losses.

Acknowledgement

We are thankful to Prof. Marc Burgelman and his group at the Department of Electronics and Information Systems (EIS), University of Gent, Belgium who developed SCAPS software used in this study and Mr. Muhammed Baba-Saje, Chemistry department, Nile University for his support during the synthesis of graphene using modified Hummer's method.

References

1. Mahajan, P., Datt, R., & Chung Tsoi, W. (2020). Recent progress, fabrication challenges, and stability issues of lead-free tin-based perovskite thin films in the field of photovoltaics. Chemical Reviews, 429, 213633.
2. Iqbal, Z. M., Ali, S. R., & Khan, S. (2019). Progress in dye-sensitized solar cells by incorporating natural photosensitizers. Solar Energy, 181, 490-509.
3. Geim, A. K., & Novoselov, K. S. (2007). The rise of graphene. Nature Materials, 6(3), 183–191.
4. Kumar, P., Divya, N., & Ratan, J. K. (2019). Synthesis and characterization of chemically derived graphene oxide from graphite. In Sustainable Engineering 85-94.
5. Paulchamy B, Arthi G, Lignesh BD (2015) A Simple approach to stepwise synthesis of graphene oxide nanomaterial. J Nanomed Nanotechnology 6(1), 253.
6. Hu, W., Yang, S., Yang, S. (2019). Surface Modification of TiO2 for PSCs. Trends in Chem. 2(2), 148-162.
7. Tress, W., Domanski, K., Hagfeldt, A. (2019). Performance of perovskite solar cells under simulated temperature-illumination real-world operating conditions. Nature Energy doi:10.1038/s41560-019-0400-8
8. Chou, J. C., Lin, Y. J., & Liao, Y. H. (2016). Photovoltaic performance analysis of DSSC with ZnO compact layer and TiO2/GO composite photoanode. IEEE Journal of Electron Devices Society, 4(6), 409.
9. Alam, S. N., Sharma, N., & Kumar, L. (2017). Synthesis of graphene oxide by modified Hummer's method and its thermal reduction to obtain reduced graphene oxide (rGO). Graphene, 6(1), 1-18.
10. Kim, K., Yoo, J. S., Ahn, S. K., Eo, Y.-J., Cho, J.-S., Gwak, J., & Yun, J. H. (2017). Performance prediction of chalcopyrite-based dual-junction TSCs. Solar Energy, 155, 167-177.
11. Elseman, A.M., Shalan, A.E., Rashad, M.M. (2017). Experimental and simulation study for impact of different halides on the performance of planar PSCs. Mat. Sci. in Semiconductor Processing, 66, 176-185.
12. Dadashbeik, M., Fathi, D., Eskandari, M. (2020). Design and simulation of PSCs based on graphene and TiO2/graphene nanocomposite as electron transport layer. Solar Energy, 207, 917-924.
13. Daraie, A., Fattah, A. (2020). Performance improvement of perovskite heterojunction solar cell using graphene. Optical Materials, 109, 110254.
14. Hummers, W.S., Offeman, R.E. (1958) Preparation of graphitic oxide, J.Am. Chem.Soc. 80, 1339-339.
15. Chou, J.C., Chang, J.X., Ko, C.C. (2020). Improving DSSC performance using enhanced double layers based on magnetic beads and RGO. IEEE Transactions on Nan, 1-1.
16. Agresti, A., Pescetelli, S., Taheri, B. (2016). Graphene-Perovskite Solar Cells Exceed 18% Efficiency: A Stability Study. Chem Sus Chem, 9(18), 2609-2619.
17. Gagandeep, Singh M., Kumar, R. (2020). Investigating the impact of layer properties on the performance of p-graphene/CH3NH3PbI3/n-csi solar cell using numerical modeling. Super-lattices and Microstructures, 106468.
18. Kumar, N., Patel, S. R., Gohel, J. V. (2018). Superior efficiency achievement for FAPbI3-perovskite thin film solar cell by optimization with response surface methodology technique and partial replacement of Pb by Sn. Optik, 176, 262-277.
19. Yang H.Y, Rho W.Y, Lee S.K. (2019). TiO2 nanoparticles/nanotubes for efficient light harvesting in perovskite solar cells, Nanomaterials 9(3), 326.
20. Marcano, D.C, Dmitry V. K, Jacob M.B (2010) Improved Synthesis of GO, ACS Nano, 4(8), 4806.
21. Hazeghi F, Ghorashi, SMB .(2019). Mater. Res. Express. Doi: 10.1088/2053-1591/ab2f1b.
22. Haidari, G. (2019). Comparative 1D opto-electrical stimulation of the perovskite solar cell. AIP Advances, 9(8), 085028.
23. Lee, K. Lin, W.J., Chen, S.H., & Wu, M.C. (2019). Control of TiO2 electron transport layer properties to enhance perovskite photovoltaics perf and st. Organic Electronics, 77, 105406.
24. Kazmi, S.A., Hameed S., Ahmed, A.S. (2016). Electrical and optical properties of graphene-TiO2 nanocomposite and its applications in DSSC, J.Alloys and Compounds, 691, 659-665.
25. Baharin A., Sahari S.K., Kemat R. (2020). The Effects of TiO2 and RGO Doping Ratio Variation to the Performance of DSSC Intl Jr of Nanoelectronics and Materials, 13(1), 159-168.
26. Eluyemi, M., Eleruja, M., Adedeji, A. (2016). Synthesis and Characterization of Graphene Oxide and Reduced Graphene Oxide Thin Films Deposited by Spray Pyrolysis Method. Graphene, 5, 143-154.
27. Jarwal, D. K., Mishra, A. K., Kumar, A. (2020). Fabrication and TCAD simulation of TiO2 nano-rods electron transport layer-based perovskite solar cells. Sup and Micr, 140, 106463.

28. Kanoun, A.A., Kanoun, M.B., Merad, A.E. (2019). Toward development of high-performance PSCs based on CH3N-H3GeI3 using computational approach. Solar Energy, 182, 237-244.
29. Kumar, M., Raj, A., Kumar, A., & Anshul, A. (2020). An optimized lead-free formamidinium Sn-based perovskite solar cell design for high power conversion efficiency by SCAPS simulation. Optical Materials, 108, 110213.
30. Paulson, P.D., Birkmire, R.W., Shafarman, W.N. (2003). Optical characterization of CuIn1−xGaxSe2 alloy thin films by spectroscopic ellipsometry. J. App Phy, 94(2), 879-888.
31. Wali, Q., Elumalai, N. K., Iqbal, Y., Uddin, A., Jose, R. (2018). Tandem perovskite solar cells. Renewable and Sustainable Energy Reviews, 84, 89–110.
32. Ladan H.M.A and Buba A.D.A. (2021). Synthesis and Characterization of Graphene for Perovskite Solar Cells, Ph.D Thesis, Department of Physics, Faculty of Science, University of Abuja, Nigeria. www.uniabuja.edu.ng.
33. Burgelman M., Nollet P., Degrave S. (2000). Modeling polycrystalline semiconductor solar cells, Thin Solid Films, 527-532.
34. Lakhdar, N., Hima, A. (2019). Electron transport material effect on performance of perovskite solar cells based on CH3NH3GeI3. Optical Materials, 109517.
35. Rao H., S. Ye, W. Sun, W. Yan, Y. Li, H. Peng, Z. Liu, Z. Bian, Y. Li, C. Huang, (2016) Nano Energy solar cells by an effective Cl doping method. 27, 51-57.
36. Rai, S., Pandey, B. K., Dwivedi, D. K. (2020). Modeling of highly efficient and low cost CH3NH3Pb(I1-xClx)3 based PSCs by numerical simulation. Optical Mat., 100, 109631.
37. Zhu Z., Y. Bai, X. Liu…A.K.Y. Jen, (2016) Enhanced efficiency and stability of inverted PSCs using highly crystalline SnO2 nanocrystals as the robust electron-transporting layer, Adv. Mater. 28, 6478-6484.
38. Karthick, S., Velumani, S., Bouclé, J. (2020). Experimental and SCAPS simulated formamidine perovskite solar cells: A comparison of device performance. Solar Energy, 205, 349-357.
39. Sutar D.S, G. Singh and V. D. Botcha. (2012). Electronic structure of graphene oxide and reduced graphene oxide monolayers", Appl. Phys. Lett., 101, 103103.
40. Wang, H., Wang, X., … Zong, X. (2020). Organic-Inorganic Hybrid Perovskites: Game-Changing Candidates for Solar Fuel Production. Nano Energy, 104647.
41. Mandadapu U, S.V. Vedanayakam, K. Thyagarajan, Simulation and analysis of lead-based perovskite solar cell using SCAPS-1D, Indian J. Sci. Technol. 10, 1-8.
42. Zhang, P., Yang, F., Kamarudin.Hayase, S. (2018). Performance enhancement of mesoporous TiO2-based PSCs by SbI3 interfacial modification layer. ACS App Mat. & Interfaces, 10(35), 29630–29637.
43. Zhou, Y., Chen, J., Bakr, O. M., Sun, H.-T. (2018). Metal-doped lead halide perovskites: synthesis, properties, and optoelectronic applications. Chemistry of Materials, 30(19), 6589–6613.
44. Mudd, G. W., Svatek, S. A. Pattani, A. (2015). High Broad-Band Photoresponsivity of Mech Formed InSe-Graphene van der Waals Heterostructures. Adv. Mat, 27(25), 3760-3766.